Biol. Cybern. 91, 347–358 (2004)
DOI 10.1007/s00422-004-0530-2

Biological Cybernetics

Continuum limit of discrete neuronal structures: is cortical tissue an "excitable" medium?

J. L. van Hemmen*

Department of Mathematics, The University of Chicago, Chicago, IL 60637, USA
and Physik Department der TU München, 85747 Garching bei München, Germany (*permanent address*)

Received: 6 May 1996 / Accepted: 15 October 2004 / Published online: 12 November 2004

Abstract. As a simple model of cortical tissue, we study a locally connected network of spiking neurons in the continuum limit of space and time. This is to be contrasted with the usual numerical simulations that discretize both of them. Refractoriness, noise, axonal delays, and the time course of excitatory and inhibitory postsynaptic potentials have been taken into account explicitly. We pose, and answer, the question of whether the continuum limit presents a full description of scenarios found numerically (the answer is *no*, not quite). In other words, can the numerics be reduced to a continuum description of a well-known type? As a corollary, we derive some classical results such as those of Wilson and Cowan (1973), thus indicating under what conditions they are valid. Furthermore, we show that spatially discrete objects may be fragile due to noise arising from the stochasticity of the individual neurons, whereas they are not once the continuum limit has been taken. This, then, resolves the above question. Finally, we indicate how one can directly incorporate orientation preference of the neurons.

1 Introduction

By itself, a neuron can be imagined as an excitable element. Here we pose, and answer, the question of whether a large number of locally connected neurons can be described as an *excitable* medium (Levin and Segel 1985; Tyson and Keener 1988; Murray 1989), a continuous structure; see also Cross and Hohenberg (1993) and Meron (1992) for a wealth of additional information. Following Murray, we define a medium to be "excitable" if a stimulus of sufficient size can initiate a traveling pulse that will propagate through the medium.

Our motivation to study this type of problem is a simple and natural one. By now we know (Fohlmeister et al. 1995) what *spontaneous* collective excitations can exist in a spatially discrete network of spiking neurons, i.e., of neurons on a two-dimensional lattice. Both lateral excitation and inhibition have been included. The model, which will be sketched in Sect. 2, has been devised so as to describe a piece of tissue in the primary visual cortex. Our interest in this type of system stems from both the strong simplifications made possible by studying spontaneous excitations, i.e., without external retinal input, and the availability of experimental data provided by hallucinations.

The underlying hypothesis was, and is, that the "form constants" that occur in hallucinations (Klüver 1966; Siegel and West 1975; Siegel 1977; Cowan 1985) are generated in the primary visual cortex. If this is true, our considerations allow a direct check, which we have exploited elsewhere. Increasing the strength A of the excitatory interactions and starting each time with random initial conditions, we have found four scenarios, which are displayed below (Figs. 1–4). So A is a kind of bifurcation parameter. For A low, the only state is a low-activity one, with incoherently firing neurons. It is not very interesting and, hence, will be discarded most of the time. As A increases, we obtain (i) moving stripes, (ii) rotating spirals and broad moving bands, which may coexist, (iii) growing rings, which may form a so-called tunnel, and (iv) complex pulsating patterns. It is to be stressed, though, that the study of spontaneous excitations under the influence of hallucinogens is not at stake here. We take them as an example of what can be described mathematically by suitable models and concentrate on the question of how these behave in the *continuum* limit. The numerical simulations are used as a mere illustration.

The second and third scenarios, spirals and rings, are well known from the theory of excitable media. So a natural question is whether we can interpret a highly connected set of neurons as an excitable medium, the key difference

Correspondence to: J. L. van Hemmen
(e-mail: Leo.van.Hemmen@ph.tum.de, Tel.: +49-89-28912362 (office), +49-89-28912380 (secretary), Fax: +49-89-28912296)

* This paper was written while the author spent a sabbatical at the University of Chicago. For reasons beyond our control the manuscript remained as such for quite a while. In the meantime the continuum limit has become a hot topic. The present approach complements what is available at the moment so that its publication may well turn out to be a valuable service to the scientific community.

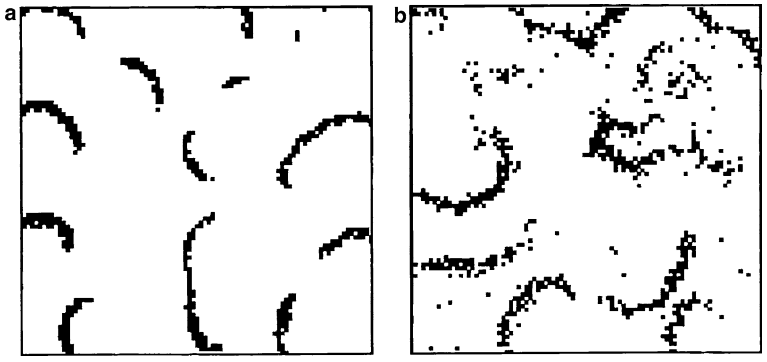

Fig. 1a,b. Scenario I – Stripes. **a** 90 × 90 network with locally homogeneous couplings $\hat{A} = 0.16$, $\hat{B} = 0.02$, while $r_0 = 15$ and $r_{\max} = 20$; cf. (8). **b** 90 × 90 network with locally sparse, excitatory couplings whose probability decreases with distance; cf. Sect. 2. Here $\lambda_{\text{Gauss}} = 2$ and $D = 0.056$. Note the similarity of the two figures despite their different microscopic structures. For all figures we have taken random initial conditions. The parameter values will be explained shortly. Taken from Fohlmeister et al. (1995), whom one may consult for all details concerning the numerics

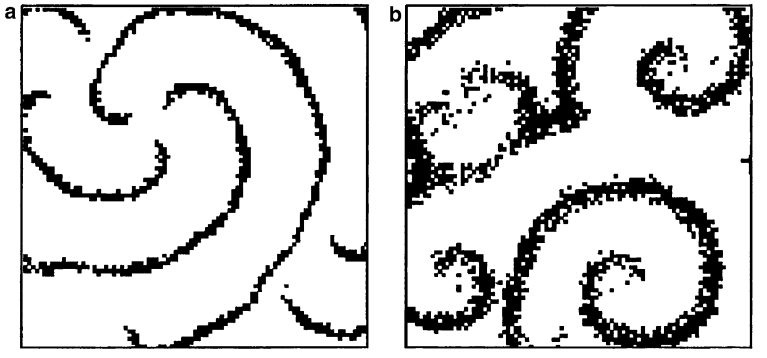

Fig. 2a,b. Scenario II – Spirals. **a** 90 × 90 network with $A = 0.12$, $B = 0.02$, $\lambda_1 = 15$, and $\lambda_2 = 100$; cf. (7). Two or more spirals may coexist as shown in **b** where we have a 90 × 90 network with excitatory couplings whose probability decreases with distance; cf. Sect. 2. Here $\lambda_{\text{Gauss}} = 2.83$ and $D = 0.1$. Taken from Fohlmeister et al. (1995)

between neurons and an excitable medium being that the former constitute a *discrete* structure – in simulations both in space and in time – whereas the latter handles space-time as a continuum. Though the similarities as they show up in scenarios II and III are evident, nonstandard scenarios such as I and IV already hint at characteristics of neuronal structures.

In what follows we analyze the continuum limit in detail. In Sect. 2 we list the "wetware" of cortical tissue and spell out the details of the Spike Response Model (Gerstner and van Hemmen 1992, 1993, 1994; Gerstner et al. 1993), which was used in the simulations and is the starting point of the present considerations. It may be well to realize that the model incorporates both the axonal delays and the (linear) response of the dendritic tree and the firing characteristics of the hillock, i.e., its refractory behavior and a threshold. An incoming spike lasts for about 1 ms. Since it is convolved with a dendritic response function that has a characteristic time constant of *several* milliseconds, the precise form of the spike is not very important and its effect is that of a(n approximate) delta function. In Sects. 3 and 4 we analyze and perform the continuum limit both in space and in time for two models that are, on the one hand, slightly different from, but on the other hand more general than, the one used in the numerics. They also differ from those studied by Gerstner (1995), who treated the continuum limit in time from a rather different point of view. As a corollary we derive some classical results such as those of Wilson and Cowan (1973), thus indicating under what conditions they are valid. The symmetries of the model and their consequences for bifurcation behavior are studied in Sect. 5. Orientation preference of the neurons is incorporated into the formalism in Sect. 6. A discussion can be found at the end of this paper. In view of the complexity of the material, our approach is sometimes bound to be somewhat formal, but, as a payoff, this will allow us to clearly isolate the problems associated with the continuum limit and its implicit neglect of the inherent stochasticity of *discrete* elements such as biological neurons.

Relevant as the issue may be, derivations of a continuum limit for spiking neurons are rare; in fact, they are nonexistent. I can only mention an ansatz of Feldman and Cowan (1975). The early work of Cowan (1968) and An der Heiden (1980) refers to a rate instead of a spike coding. The reader is referred to the latter for a more detailed account of the various aspects of a rate coding.

Before proceeding we would like to point out some similarities with and differences between a recent paper by Milton et al. (1995) and the present work. Both analyze activity waves in neuronal networks. Strikingly, Milton et al. start by writing down continuum equations and then question how these might be approximated by a discrete structure, whereas we do it just the other way around and start with discrete neurons. Furthermore, they consider a neuron as a leaky integrator, whereas we employ arbitrary dendritic response functions and include axonal delays. In addition, we do not assume any a priori distribution of excitation, whereas in the case of Milton et al. a Poisson distribution is lurking in the background. Finally, lateral inhibition is handled completely differently: in their case it does not exist, whereas in our case we may have a strong, or even a shunting, inhibition. Both approaches, however, do incorporate neuronal refractory behavior.

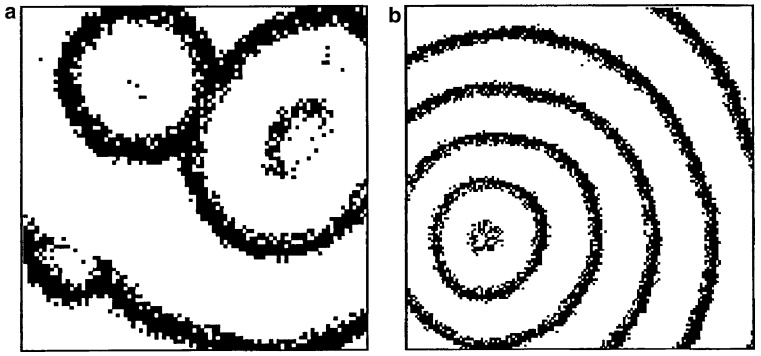

Fig. 3a,b. Scenario III – Rings. **a** 90×90 network with $A = 0.14$, $B = 0.02$, $\lambda_1 = 15$, and $\lambda_2 = 100$; cf. (7). The two rings annihilate each other where they meet. New rings originate from the two centers. In **b** we show a 150×150 network with excitatory couplings whose probability decreases with distance; cf. Figs. 1b and 2b. Here $\lambda_{\text{Gauss}} = 2.83$ and $D = 0.12$. Taken from Fohlmeister et al. (1995)

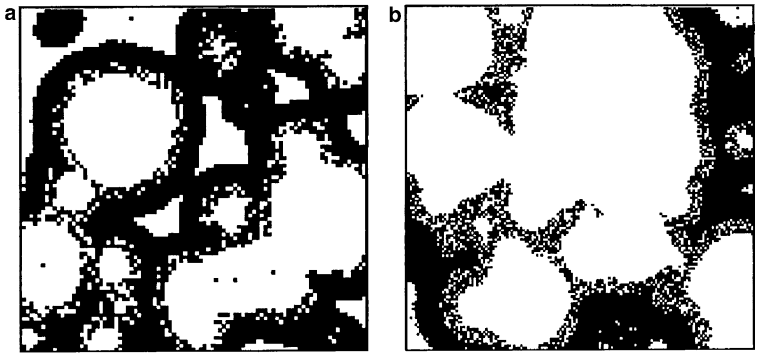

Fig. 4a,b. Scenario IV – Collective burst. **a** 90×90 network with $A = 2.4$, $B = 0.02$, $\lambda_1 = 8.4$, and $\lambda_2 = 100$; cf. (7). **b** 150×150 network with excitatory couplings whose probability decreases with distance; cf. Figs. 1b–3b. Here we have an exponential distribution with $\lambda_{\text{exp}} = 3$. Furthermore, $D = 0.14$. Taken from Fohlmeister et al. (1995)

2 Neurons on a lattice: spike response model

The essentials of neuronal behavior are the absolute and relative refractory period, the response at the soma resulting from synaptic input (here described by a dendritic response function, in short, an alpha function), the omnipresent delays, and noise. All these ingredients have been incorporated into the Spike Response Model (Gerstner and van Hemmen 1992, 1993, 1994; Gerstner et al. 1993). It presents a faithful but simplified description of the neurons themselves *without* recourse to differential equations. This is an essential simplification if we want to perform a numerical simulation of the spatiotemporal activity of a large system of neurons (say, $N \geq 10^6$) with a realistic response (alpha) function over a long period of time.

In addition, the Spike Response Model allows for a direct treatment of noise arising from either inherent uncertainties existing in the neuronal firing mechanism, i.e., intrinsic noise, or "fluctuating" synapses that may, but need not, transmit a spike (Rosenmund et al. 1993; Hessler et al. 1993). Though an application of the arguments below to a pure differential equation description à la Hodgkin and Huxley is straightforward, the incorporation of intrinsic noise into the very same description is not. In fact, it is an open problem. On the other hand, fluctuating synapses are relatively easy to handle, and we therefore refrain from treating them here.

For the moment, we discretize time by units $\Delta t = 1$ ms, the width of a spike, and label the neurons on a two-dimensional square lattice by the index i. The lattice distance is a, and we start with $a = 1$ (in units of, say, 10μm). The state of a neuron is described by $S_i \in \{0, 1\}$. If the potential h_i at the hillock of neuron i reaches the threshold ϑ, then the neuron is expected to fire. We describe this stochastic behavior through a transition probability

$$\text{Prob}\{S_i(t + \Delta t) = 1 | h_i(t)\} = \phi[\beta(h_i(t) - \vartheta)], \tag{1}$$

where ϕ is a function of a real variable with a range between 0 and 1. Equation (1) represents the conditional probability that neuron i will fire at time $t + \Delta t$ given $h_i(t)$. It does so *independently* of the other neurons. For the sake of definiteness we assume that in the noise-free limit $\beta \to \infty$ we get $S_i(t + \Delta t) = \Theta[h_i(t) - \vartheta]$, where Θ is the Heaviside step function: $\Theta(x) = 1$ for $x > 0$ and $\Theta(x) = 0$ for $x < 0$. Hence ϕ has a somewhat restricted asymptotic behavior. The ensuing arguments do not depend on this assumption and are, in fact, quite general. In the numerics to be specified shortly we have taken $\vartheta > 0$ and

$$\phi(x) = \frac{1}{2}(1 + \tanh x)\,. \tag{2}$$

In passing we note that the past of the neuron has been incorporated into $h_i(t)$ – indeed, at time t. (See below.) We henceforth absorb ϑ into ϕ. Furthermore, if noise were to be dominantly generated by fluctuating synapses, then the above prescription (1) with ϕ Gaussian and β replaced by some other parameter is still correct. Plainly, a Gaussian does not satisfy the above monotonicity requirement exemplified by (2). In the numerics leading to Figs. 1–5, $\beta = 25$ while $\vartheta = 0.12$.

The Spike Response Model describes the response of a neuron – both as sender and as receiver – to a spike. If a neuron has fired a spike, it exhibits refractory behavior, i.e., it cannot spike or only hardly spikes. This is taken care of by the refractory function η, which is, say, $-\infty$ during

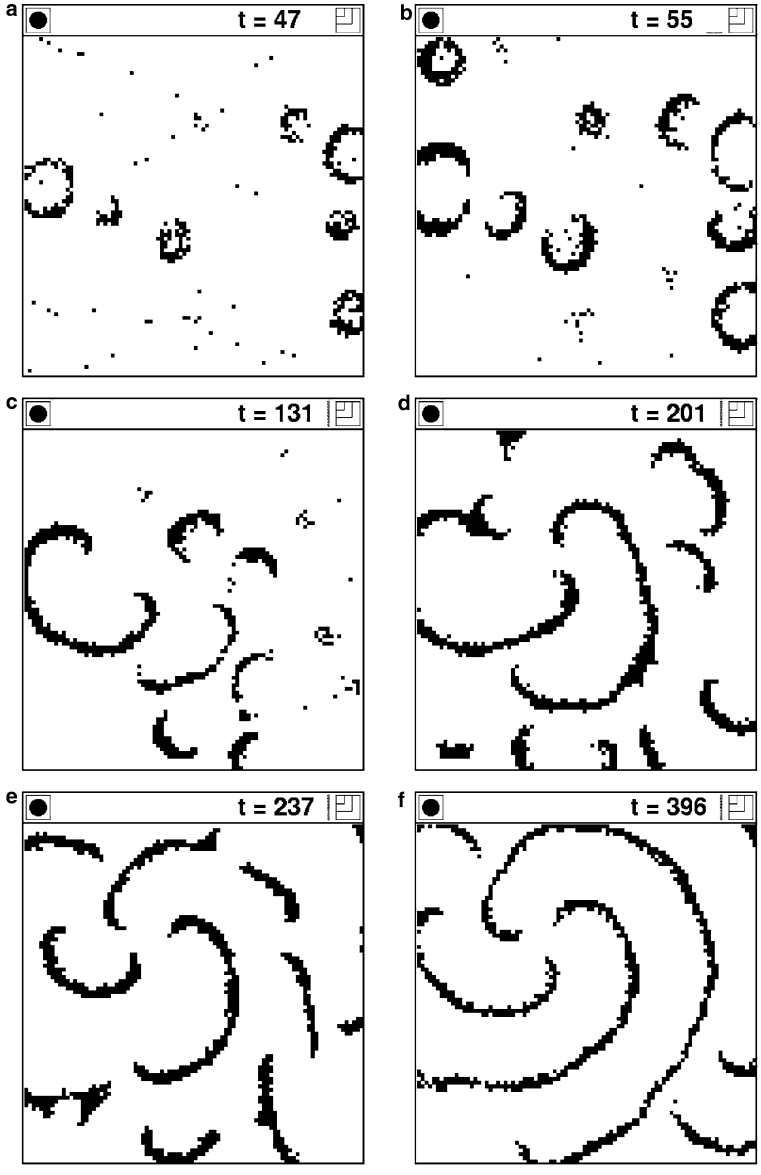

Fig. 5a–f. Scenario II, a sequence of patterns leading to Fig. 2a. The pictures **a**–**f** are taken at subsequent times 47–396 ms, as indicated above them. In **a** we see rings emanating from various centers. They have a *finite* thickness and grow in a *discrete* structure so that there is a finite probability that a hole will appear. As one sees, this is indeed the case: the rings are fragile, **b** break up, **c** form stripes, and **d, e** reorganize themselves so as to build a spiral (**e**). It is not necessary that the spiral have three arms. Taken from Fohlmeister (1994)

the absolute refractory period and negative but increasing to zero thereafter:

$$h_i^{\mathrm{refr}}(t) = \sum_{s \geq 0} \eta(s) S_i(t-s)\,. \tag{3}$$

For instance, in the simulations we have taken $\eta(s) = -\infty$ for $s = 1$ and zero elsewhere. By varying η one can simulate nearly any neuron (Gerstner and van Hemmen 1992; Kistler et al. 1997).

The spike travels along an axon leaving neuron j and reaches a synapse on the dendritic tree of neuron i after Δ_{ij} ms. Let the synaptic strength be J_{ij} and denote i's dendritic response function by ε. Then we obtain for the total synaptic input at the hillock of neuron i

$$h_i^{\mathrm{syn}}(t) = \sum_j J_{ij} \sum_{s \geq 0} \varepsilon(s)\, S_j(t-s-\Delta_{ij})\,, \tag{4}$$

where, e.g., $\varepsilon(s) = s\tau_\varepsilon^{-2} \exp(-s/\tau_\varepsilon)$. A typical value is $\tau_\varepsilon = 2$ ms, which has been adopted for the numerics. Here we take $\Delta_{ij} = \Delta(r_{ij})$, where $r_{ij} = \|i - j\|$ is the Euclidean distance. The function Δ describes a temporal delay and thus increases, e.g., linearly, as the distance r goes to infinity; of course, $\Delta(0) = 0$. One might think that delays will play a negligible role in that a few milliseconds' difference cannot influence the stability of, e.g., a collective excitation. This, however, is wrong (Gerstner et al. 1996): they do.

The neurons considered so far are pyramidal cells. These have both short- and long-range interactions. On the other hand, e.g., stellate cells (Braitenberg and Schütz 1991) have only short-range interactions and exert a rather strong influence or even an inhibitory veto on their pyramidal neighbors (Kandel and Schwartz 1985, Sect. 48). For the moment we simplify the whole structure through an inhibitory loop that is assigned to each "pyramidal" neuron (Gerstner et al. 1993; Gerstner and van Hemmen 1994; Fohlmeister et al. 1995),

$$h_i^{\text{inh}}(t) = \sum_{s \geq 0} \varepsilon^{\text{inh}}(s)\, S_i(t - s - \Delta_i^{\text{inh}})\,. \tag{5}$$

For example, in Figs. 1–4, $\varepsilon^{\text{inh}}(s)$ first assumes a (strongly) negative value for 5 ms and then decays exponentially with a time constant τ_{inh} of the order of 6 ms. The idea behind the inhibitory loop in (5) is that stellate cells operate locally. Hence we assume a *strictly* local interaction; for details, see Gerstner et al. (1993). In a continuum limit one cannot but fix $\Delta_i^{\text{inh}} = \Delta^{\text{inh}}$ so that there is no – or a very weak – dependence upon i. In Sect. 4 we will model the stellate cells explicitly and incorporate them into a spatial structure. Putting things together we obtain

$$h_i(t) = h_i^{\text{refr}}(t) + h_i^{\text{syn}}(t) + h_i^{\text{inh}}(t)\,, \tag{6}$$

which is to be substituted into (1) so as to generate $S_i(t + \Delta t)$ and, thus, the dynamical evolution. What is left is specifying the J_{ij} in (4).

For the sake of general theory we need only require $J_{ij} = J(r_{ij})$, where $r_{ij} = \|i - j\|$ is the Euclidean distance between i and j. A widely used example, whose merits and faults need not be discussed here, is a "Mexican hat" interaction,

$$J_{ij} = A \exp(-r_{ij}^2/\lambda_1) - B \exp(-r_{ij}^2/\lambda_2)\,, \tag{7}$$

with $\lambda_1 \ll \lambda_2$ and $A \gg B$. A second possibility, which we have also studied, is

$$J_{ij} = \hat{A} \text{ for } r_{ij} \leq r_0 \text{ and } -\hat{B} \text{ for } r_0 < r_{ij} \leq r_{\max}\,, \tag{8}$$

with J_{ij} vanishing beyond $r_{\max}$ and, again, $\hat{A} \gg \hat{B}$. We use free (natural) boundary conditions throughout. In our numerical simulations we have seen no difference between (7) and (8). Alternatively, and giving rise to the very same scenarios, one can replace J_{ij} in (4) by $D\tilde{J}_{ij}$, where $\tilde{J}_{ij} = 1$ with probability $p(r_{ij}) = \exp[-(r_{ij} - 1)/\lambda_{\text{exp}})]$ or $\exp -[(r_{ij} - 1)/\lambda_{\text{Gauss}})]^2$; otherwise, $\tilde{J}_{ij}$ vanishes. Typical values for the λs were in the range between 2 and 5, the lattice distance being $a = 1$. The probabilities have been chosen in such a way that the nearest neighbors ($r_{ij} = 1$) are always connected. D is a drug parameter, comparable to A. Both are considered as bifurcation parameters that determine what *spontaneous* collective excitations may exist. Hence we do not include inputs, which could be added trivially but whose realistic modeling is highly nontrivial.

Summarizing, we have explicitly modeled the various interactions including inhibitory stellate cells, the delays that are abundantly present in the cortex, dendritic neuronal response, and noise. We now turn to the continuum limit of the network behavior as it shows up, for example, in Figs. 1–4 for discrete neurons.

3 Continuum limit

In the present context, taking a continuum limit means that we allow both the lattice constant a and the time discretization Δt to go to zero, keeping the synaptic input and the number of spikes per individual neuron finite and restricting the time t to a finite and fixed interval. The key idea is intuitively that in the continuum limit more and more neurons enter the scene (so that one has to rescale the interactions) and their behavior continuously interpolates between fully active (black) and quiescent (white). This means that the field $h(\mathbf{x}, t)$ is continuous both in $\mathbf{x}$ and in t. As long as ϕ_β is smooth, we conclude from (17) and the more general (24) and (25) below, which describe the system *after* the continuum limit has been taken, that this continuity indeed holds. This will be assumed throughout what follows.

3.1 Setup of the continuum limit

We will proceed somewhat formally and begin by studying the continuum limit of a rather simple system where each neuron has an inhibitory loop with delay Δ^{inh}. The synaptic contribution (4) from the other pyramidal cells can be written

$$h_i^{\text{syn}}(t) = \sum_{s \geq 0} \varepsilon(s) \left[\sum_j J_{ij} S_j(t - s - \Delta_{ij}) \right]. \tag{9}$$

The sum over j in the square brackets is, typically, over $n \approx 10^4$ neurons. If Δ_{ij} did not depend on j, then we could apply the strong law of large numbers (Lamperti 1966; Breiman 1968) directly so as to conclude that the very many terms, which are taken at different sites at the same time, can be replaced by their nonzero average and neglect the (Gaussian) noise generated by the fluctuations, the deviations from the mean. This is the key idea: once the mean ϕ is nonzero we can take advantage of the strong law of large numbers so as to get a deterministic synaptic input. [This is a bit subtle in that one has to apply a sublattice argument (Riedel et al. 1988) to the two sets of active and inactive neurons in order to generate the required homogeneity in $h_i^{\text{syn}}(t - s - \Delta_{ij} - 1)$]. In the continuum limit with $n \to \infty$, the above argument becomes exact. For the original system we started with, we can assume that it is nearly exact since each neuron interacts with about $n \approx 10^4$ other neurons. We now turn to the mathematical details.

Since Δ_{ij} varies slowly with j, we obtain a good approximation for the original system and exactly in the continuum limit as $n \to \infty$ that the S_j in the sum (9) can be replaced by their deterministic average $\phi(\beta h_j)$.[1] Thus, dropping the fluctuation term and replacing t by $t + \Delta t$ in (9), we end up with the average of (9):

[1] In this form, the strong law of large numbers cannot be used in, e.g., the Hopfield model, which is characterized by an extreme correlation between the J_{ij} and the activity patterns. By the very nature of the Hopfield model, however, a continuum limit would be senseless since its patterns, the fixed points to be of the dynamics, are generated by *independent* identically distributed stochastic variables ξ_i^μ assuming the values ± 1 with equal probability and, thus, do not allow a continuum limit.

$$h_i^{\mathrm{syn}}(t+\Delta t)=\sum_{s\geq 0,\, j}\varepsilon(s)J_{ij}\phi[\beta h_j(t-s-\Delta_{ij})]\,. \tag{10}$$

So much for the synaptic input. In biophysical terms, (10) is a mean-field ansatz that is nearly exact once the activity is nonzero. The underlying argument is the strong law of large numbers (Breiman 1968). In this way we have moved from a spike to a rate coding. Given ϕ and η, it is a simple task to compute a neuron's firing rate for a constant input (Gerstner and van Hemmen 1992).

The inhibitory loop (5) at time $t+\Delta t$ gives rise to the simple-looking term

$$\sum_{s\geq 0}\varepsilon^{\mathrm{inh}}(s)S_i(t+\Delta t-s-\Delta^{\mathrm{inh}})\,, \tag{11}$$

while the refractory field at i produces a contribution that seems equally simple:

$$\sum_{s\geq 0}\eta(s)S_i(t+\Delta t-s)\,. \tag{12}$$

Well, are they really that simple? The S_i are Boolean variables assuming only two values, viz., 0 and 1. As such, they can never be realized as solutions of a differential equation without singularities, e.g., delta functions. We therefore consider a *little* "square" around $i:=\mathbf{x}$ with $|V_{\mathbf{x}}|$ elements, average over all sites of the square, which is reasonable in view of the type of solution we are aiming at, viz., that of Figs. 1–4, and replace the local variables S_i by

$$|V_{\mathbf{x}}|^{-1}\sum_{\mathbf{y}\in V_{\mathbf{x}}}S_{\mathbf{y}}(t+\Delta t)\longrightarrow|V_{\mathbf{x}}|^{-1}\sum_{\mathbf{y}\in V_{\mathbf{x}}}\phi_\beta[h(\mathbf{y},t)]\,. \tag{13}$$

This smooths the solution we are looking for and, hence, will be called *smoothing*. To concentrate on the argument of ϕ, we have promoted β to the status of an index. It henceforth has a fixed but finite value. I would like to stress that we cannot but invoke the above "interpolation" so as to smooth the strictly local refractory behavior; there is no way out. In a sense, smoothing is a fundamental weakness of the continuum limit.

What to do with the sum on the right in (13)? For any smooth function f and the four nearest neighbors of $\mathbf{x}$ along the x and y axes, we would find a discretized version of the Laplacian Δ for lattice spacing a:

$$|V_{\mathbf{x}}|^{-1}\sum_{\mathbf{y}\in V_{\mathbf{x}}}f(\mathbf{y})=f(\mathbf{x})+\frac{a^2}{4}\Delta f(\mathbf{x})+\mathcal{O}(a^4)\,. \tag{14}$$

Four neighbors are no good yet for applying the strong law of large numbers, but it is plain that one can use more elaborate averages so as to find (14) or an equivalent thereof. It is also plain that the continuum limit with $n\to\infty$ makes the argument exact. In view of (6) taken at time $t+\Delta t$, we now end up with

$$\begin{aligned}\tau\frac{\partial h(\mathbf{x},t)}{\partial t}&=-h(\mathbf{x},t)\\&\quad+a^{-2}\tau^{-1}\int ds d\mathbf{y}\varepsilon(s)J(\mathbf{x}-\mathbf{y})\Phi_\beta(\mathbf{x},\mathbf{y},t-s;\Delta)\\&\quad+\tau^{-1}\int ds\,\varepsilon^{\mathrm{inh}}(s)\phi_\beta[h(\mathbf{x},t-s-\Delta^{\mathrm{inh}})]\\&\quad+\tau^{-1}\int ds\,\eta(s)\,\phi_\beta[\,h(\mathbf{x},t-s)]+\mathcal{R}\,,\end{aligned} \tag{15}$$

where for the sake of notational simplicity

$$\Phi_\beta(\mathbf{x},\mathbf{y},t-s;\Delta):=\phi_\beta[h(\mathbf{y},t-s-\Delta(\|\mathbf{x}-\mathbf{y}\|))]\,. \tag{16}$$

Furthermore, $\tau=\Delta t=1$ ms and $\mathcal{R}$ represents the second derivatives that occur in (14). The latter are in good company since they have a^2 as a prefactor. Two additional remarks are in order. First, in a discrete description we can define η to be $-\infty$ during the absolute refractory period, which is sampled exactly by $S_i=1$ during a spike and $S_i=0$ otherwise so that $0\times\infty$ gives no contribution. If we replace S_i by $\phi_\beta(h_i)$, we have to take care of the singularity of η by assigning to η a *finite* minimum so that $\eta(s)\phi_\beta[\,h(\mathbf{x},t-s)]$ is negligible once $\phi_\beta[\,h(\mathbf{x},t-s)]$ has returned to the "inactive" state. After all, nothing has to be sampled anymore. Second, if the density of the neurons is inhomogeneous, we simply add a density function $\rho(\mathbf{y})$ to J in the first integrand of (15).

3.2 Continuum limit proper

We have to perform the continuum limit $a\to 0$ in conjunction with $\tau\to 0$. As for space, packing more and more neurons into a certain fixed volume one would increase the density and, hence, the amplitude of the input signals indefinitely. This is to be compensated by, e.g., weakening J through the substitution $J\to a^2J$. For smooth solutions, the term $\mathcal{R}$ disappears from (15) in the limit $a\to 0$.

As for time, the key question is: What to do with the dimensionless fraction $\tau/\partial t$ in the left-hand side of (15)? There are at least two ways out. The first is keeping $\tau>0$, say, $\tau=1$ ms, as a prefactor of the differential operator. The second, and preferable, way is to rescale *all* time variables by $\tau^{-1}t\to t$ and redefine the functions h, ε, and η by putting $h(\mathbf{x},\tau t)\to h(\mathbf{x},t)$, and so on. The τs on the left and on the right then drop out.

Whatever rescaling procedure we take, for a given neuron density ρ we arrive at

$$\begin{aligned}\frac{\partial h(\mathbf{x},t)}{\partial t}&=-h(\mathbf{x},t)\\&\quad+\int ds d\mathbf{y}\,\varepsilon(s)\rho(\mathbf{y})J(\mathbf{x}-\mathbf{y})\Phi_\beta(\mathbf{x},\mathbf{y},t-s;\Delta)\\&\quad+\int ds\varepsilon^{\mathrm{inh}}(s)\phi_\beta[h(\mathbf{x},t-s-\Delta^{\mathrm{inh}})]\\&\quad+\int ds\eta(s)\phi_\beta[h(\mathbf{x},t-s)]\,.\end{aligned} \tag{17}$$

We note that the above equation is in the style of Hopfield (1984). A similar equation for the fraction of time X_r when neuron r is not refractory, a rate description, dates back

to Cowan.[2] One has to realize, though, that in the present case, (17) has been derived with the dynamics of *spiking* neurons as a starting point.

It is now an easy matter to understand why the noise arising from the stochastic fluctuations in (9) can be dropped. The argument is the following. The average of (9), which is (10), amounts to

$$h_i^{\text{syn}} = \sum\nolimits_{s\geq 0,\, j} \varepsilon(s)\, J_{ij}\phi(\beta h_j)\,.$$

Here we have suppressed all temporal arguments. The sum is of the order n times a spatial mean $\langle\phi(\beta h)\rangle$. Deviations from the mean are approximately Gaussian. The mean should therefore be compared with the square root of the variance

$$\sum_{s\geq 0, j} \varepsilon^2(s)\, J_{ij}^2\, \phi(\beta h_j)[1-\phi(\beta h_j)]\,, \tag{18}$$

which itself is also of the order n times a small factor since typically $\phi(\beta h_j)$ in $\phi(\beta h_j)[1-\phi(\beta h_j)]$ is either near 0 or near 1 so that the only appreciable contribution stems from a narrow region around the contours, where ϕ changes from 0 to 1, or, conversely, from 1 to 0. Contours have measure zero as compared to the surface area of the excitations. The narrow region surrounding them has a small area as compared to the surface that they enclose. Furthermore, in the continuum limit with $a\to 0$ we have to rescale J_{ij}. The integrand contains J_{ij}^2, and we thus get an extra a^2 approaching zero. The variance converging to zero, we end up with (10).

Up to now we have considered the synaptic strengths as given deterministic quantities. At the end of Sect. 2 we discussed a stochastic model where $\tilde{J}_{ij}=1$ with probability $p(r_{ij})$, and $\tilde{J}_{ij}=0$ otherwise. The pictures on the right-hand side of Figs. 1–4 suggest that a continuum limit is well defined and similar to the one already discussed. Indeed, it is. Here, too, the key argument is the strong law of large numbers (Breiman 1968) , this time applied to the sampling of the bonds. We can do so since the *global* activity pattern is *not* correlated with the random bond structure – as illustrated by Figs. 1–4. Exactly as in the deterministic case, more and more neurons enter the interaction range of a specific neuron so that the strong law of large numbers applies as soon as the mean values of the $\tilde{J}_{ij}$, viz., the $p(r_{ij})$s, are nonzero. They are. The upshot of the present discussion is, then, that we can perform the substitution $J_{ij}\to Dp(r_{ij})$. The new interaction is deterministic and of the form we already discussed: $J(r_{ij})$, as advertised.

3.3 Comparison with large-scale numerics

To see the relation with the numerics discussed above, we define the variable $E(\mathbf{x},t):=\phi_\beta[h(\mathbf{x},t)]$. The function ϕ varies between 0 (white) and 1 (black) and assumes "gray" values indicating the amount of activity in between. The Figs. 1–5 representing discrete neurons show black and white only since the state variable S_i assumes only two values, viz., 0 and 1. The variable $E(\mathbf{x},t)$ is indispensable in plotting spatiotemporal activity of the excitatory (E) pyramidal cells. It smooths the boundaries between black and white. In other words, it interpolates between black and white.

Scenarios II and III are typical representatives of what is to be expected in an "excitable medium." What, however, about scenarios I and IV? The physics of scenario IV is simple. We start with a set of *discrete* neurons that are *all* inactive, i.e., with a "white" plane. Due to a steadily decreasing inhibition and the fact that neurons are stochastic elements, sooner or later a few of them will start firing. Scenario IV requires an uppercase A so that the excitation is high. Hence these neurons ignite the system and a "firestorm" rushes through it; cf. Fig. 4. The inhibition that follows vetos any activity, and we end up with a totally inactive network, i.e., with a white plane again. As time proceeds the shunting inhibition decreases. Once again some neurons will start firing – and so on. In other words, we are going to obtain a (set of coupled) nonlinear integrodelay differential equation(s) as specified below and should add some noise *by hand*. In scenarios II and III the noise can be dropped. Because of the local inhibition it is bound to vanish behind the wave fronts anyway. It is essential, however, to IV so as to allow the system to evolve in a "natural" way. Otherwise it might get stuck on a "whitish" plane. Scenario I is going to illustrate that finite objects in a noisy discrete structure are *fragile*; we return to fragility in Sect. 7.

3.4 Comparison with other work I

Despite the similarities that show up at first glance, there are several fundamental differences between the equations of Ermentrout and Cowan (1979) and ours. These authors do not allow delays, consider only the J integral in (17), and call any function of the form $\hat{f}(t)=\int ds\,\varepsilon(s)\,f(t-s)$ a "coarse-grained" version of f in the sense that it approximates f rather well. (That is correct: for smooth f we get $\hat{f}(t)\approx f(t-\tau_\varepsilon)$, where τ_ε is of the order of a few milliseconds.) Before being able to show that, in an approximate but explicit way and cutting down (17), the two formulations are equivalent we have to perform what is called a $\Sigma-\Pi$ exchange for the analog neurons of Hopfield (1984). It was already used by Ermentrout and Cowan (1980) and can be found in nearly any decent textbook on electric circuit theory. Simply stated, we have a set of differential equations

$$\dot{u}_i = -u_i + \sum_j J_{ij}\phi(u_j)\,, \tag{19}$$

with J_{ij} multiplying ϕ, and we would like to obtain an equation with ϕ *outside* the sum so that the summation and multiplication have been interchanged. To this end we suppose that the matrix J is invertible and define a vector $\mathbf{v}$ through $v_k=\sum_i (J^{-1})_{ki}u_i$. Use this in (19) so as to get

[2] See footnote 1 of his 1968 paper, which, partially in our own notation, should read: $X_r(t+\Delta t):=\varphi[\epsilon_r+\beta_r^{-1}\sum_s \alpha_{rs}X_s(t-\Delta_{rs})]$. A differential equation with $\Delta t:=\tau$ directly follows.

$$\dot{v_k} = -v_k + \phi\left(\sum_i J_{ki} v_i\right), \tag{20}$$

as desired. We now return to our original problem, (17), keep only the first two terms on the right, insert $\Delta \equiv 0$, and assume that the integral operator J, a convolution kernel, is invertible. By unitary equivalence through the Fourier transformation on $\mathbb{R}^2$, this is the case if the Fourier transform of J, say, a Gaussian kernel, does not vanish. Let, then, $H = Jh$ be the equivalent of the above $\mathbf{v}$ so that

$$\frac{\partial H(\mathbf{x},t)}{\partial t} = H(\mathbf{x},t) + \int ds \varepsilon(s) \phi_\beta[\int d\mathbf{y} J(\mathbf{x}-\mathbf{y}) H(\mathbf{y}, t-s)]. \tag{21}$$

If we assume that ε is an approximate δ-function, at least on the time scale of the functions considered here (certainly in the spirit of Ermentrout and Cowan), then we are left with equations of the form

$$\frac{\partial H(\mathbf{x},t)}{\partial t} = -H(\mathbf{x},t) + \phi_\beta[\int d\mathbf{y}\, J(\mathbf{x}-\mathbf{y})\, H(\mathbf{y},t)], \tag{22}$$

as advertised. A key difference between the two approaches is that Ermentrout and Cowan start with a rate description, whereas we start with spiking neurons and then use the strong law of large numbers so as to obtain the average over the noise, i.e., ϕ, for each of them. Furthermore, we assume that inhibition (Kandel and Schwartz 1985) plays an important role. Finally, a linear combination of Gaussians such as (7) does *not* give rise to an invertible H, and it remains to be seen whether a Fredholm alternative proves that the two formulations (H and h) are equivalent.

4 Models of cortical tissue

We are going to analyze several models of cortical tissue. In all cases, our starting point is a spatially discrete structure giving rise to a continuum limit. The model that we have studied until now, viz., (17), is the simplest and will be called model $\mathcal{A}$. A second one, viz., model $\mathcal{B}$, will be introduced next. We then relate this model to that of Wilson and Cowan (1973). As before, the time t is in a fixed bounded interval.

4.1 Excitatory and inhibitory interactions

A square lattice Ł can be considered as the disjoint union of two intertwining lattices, $Ł = Ł_1 \cup Ł_2$. We put pyramidal cells on each vertex of $Ł_1$ and homogeneously assign stellate cells to, say, a quarter of the vertices of $Ł_2$. The model is finished once we have specified the couplings on and between $Ł_1$ and $Ł_2$. On $Ł_1$ we have the interaction function J_{EE} that is defined on $\mathbb{R}^2$. The pyramidal cells excite the stellate cells through J_{IE} and are inhibited by them by way of J_{EI}. The former is accompanied by a response function resembling ε in (4); the latter goes with $\varepsilon^{\mathrm{inh}}$ of (5) or a variation thereof. Of course, the EE inhibitory loop has now been dropped. We also assign an interaction J_{II} to $Ł_2$.

Finally, the range of J_{EE} can, and in the visual cortex will, exceed that of J_{EI} (Braitenberg and Schütz 1991; Sholl 1956). The J_{EE} may become negative as in (7) and (8) due to the influence of, e.g., interneurons. Typically, e.g., as in the primary visual cortex, one has an excitatory near-neighbor interaction in addition to an indirect inhibition with a slightly longer range so that the *net effect* is a "Mexican hat." Alternatively, one makes the interneurons explicit and incorporates them into J_{EI} and J_{IE}. We will discuss the range of the interactions in detail later on. Thus we end up with two equations à la (15). In the right-hand side below we then find, in self-evident notation,

$$\begin{aligned} h_E(\mathbf{x},t) &= h_{\mathrm{EE}}^{\mathrm{syn}} + h_{\mathrm{EI}}^{\mathrm{syn}} + h_E^{\mathrm{refr}}, \\ h_I(\mathbf{x},t) &= h_{\mathrm{IE}}^{\mathrm{syn}} + h_{\mathrm{II}}^{\mathrm{syn}} + h_I^{\mathrm{refr}}, \end{aligned} \tag{23}$$

where, for instance, $h_{\mathrm{EE}}^{\mathrm{syn}}$ and $h_{\mathrm{EI}}^{\mathrm{syn}}$ are the analogs of (4) and (5) operating on the pyramidal cells (E). In a similar vein to model $\mathcal{A}$, one finds that the equations of (23) give rise to a set of two coupled integrodelay differential equations for excitatory and inhibitory neurons distributed according to densities ρ_E and ρ_I,

$$\begin{aligned} \frac{\partial h_E(\mathbf{x},t)}{\partial t} &= -h_E(\mathbf{x},t) \\ &+ \int ds d\mathbf{y}\, \varepsilon(s)\, \rho_E(\mathbf{y})\, J_{\mathrm{EE}}(\mathbf{x}-\mathbf{y})\, \Phi_{\beta,E}(\mathbf{x},\mathbf{y},t-s;\Delta) \\ &+ \int ds d\mathbf{y}\, \varepsilon^{\mathrm{inh}}(s)\, \rho_I(\mathbf{y})\, J_{\mathrm{EI}}(\mathbf{x}-\mathbf{y})\, \Phi_{\beta,I}(\mathbf{x},\mathbf{y},t-s;\Delta) \\ &+ \int ds\, \eta(s)\, \phi_\beta[h_E(\mathbf{x},t-s)], \end{aligned} \tag{24}$$

where, analogously to (16),

$$\Phi_{\beta,X}(\mathbf{x},\mathbf{y},t-s;\Delta) := \phi_\beta[h_X(\mathbf{y},t-s-\Delta(\|\mathbf{x}-\mathbf{y}\|))],$$

with $X = E$ or I. Furthermore,

$$\begin{aligned} \frac{\partial h_I(\mathbf{x},t)}{\partial t} &= -h_I(\mathbf{x},t) \\ &+ \int ds d\mathbf{y}\, \varepsilon(s)\, \rho_E(\mathbf{y})\, J_{\mathrm{IE}}(\mathbf{x}-\mathbf{y})\, \Phi_{\beta,E}(\mathbf{x},\mathbf{y},t-s;\Delta) \\ &+ \int ds d\mathbf{y}\, \varepsilon^{\mathrm{inh}}(s)\, \rho_I(\mathbf{y})\, J_{\mathrm{II}}(\mathbf{x}-\mathbf{y})\, \Phi_{\beta,I}(\mathbf{x},\mathbf{y},t-s;\Delta) \\ &+ \int ds\, \eta(s)\, \phi_\beta[h_I(\mathbf{x},t-s)]. \end{aligned} \tag{25}$$

What has been said about η being finite in conjunction with (15) applies equally well to $\varepsilon^{\mathrm{inh}}$. One can allow the delay functions Δ_{XY} to depend on X and Y, the latter two being either E or I. In addition, one can straightforwardly introduce more general response functions than the ε and $\varepsilon^{\mathrm{inh}}$ studied here. These generalizations come for free; the extra amount of labor in solving the equations does not. The following theorem summarizes the present discussion.

Limit Theorem: *For a smooth ϕ_β and t in a fixed bounded interval, the continuum limit $a \to 0$ in conjunction with $\Delta t \to 0$ transforms the dynamics of the discrete model $\mathcal{B}$ into the system of delay integrodifferential equations (24) and (25).*

This finishes the construction of model $\mathcal{B}$. Equations (24) and (25) may be compared with but – as we have seen – are different from those of Ermentrout and Cowan (1979). They differ even more from those of Milton et al. (1995). Depending on the range and nature of the interactions, we see remarkable differences between the solutions, which we will study and comment elsewhere.

4.2 Comparison with other work II

It is now a straightforward task to derive the equations of Wilson and Cowan (1973), thus indicating under what conditions these equations are valid. In so doing we assume that the neurons have an absolute refractory period of r_e (or r_i) milliseconds. The continuum limit is implicitly assumed throughout. The refractory field η no longer appears, and the only input is taken to be the synaptic one. If desired, an external input is trivial to add. Let $E(\mathbf{x}, t)$ be the fraction of excitatory neurons per unit volume becoming active per unit time at position $\mathbf{x}$ and at time t. As time is discretized with $\Delta t > 0$ this notion is well defined. We then find for a small volume $V_\mathbf{x}$ around $\mathbf{x}$

$$E(\mathbf{x}, t+\Delta t) = \frac{1}{|V_\mathbf{x}|} \sum_{i \in V_\mathbf{x}} S_i(t+\Delta t)\,, \tag{26}$$

the time discretization Δt being 1 ms. By the strong law of large numbers the weighted sum equals the expectation value of the event that a neuron at $\mathbf{x}$ fires at time $t+\Delta t$ and did *not* fire during r_e milliseconds before so as to take care of the absolute refractory period. The firing probability, once the absolute refractory period is over, is determined by the synaptic input h^{syn} only and equals $\phi_\beta[h_E^{\mathrm{syn}}(\mathbf{x}, t)]$. The probability of not firing r_e milliseconds before is $\prod_{t-r_e<s\le t}\{1-\phi_\beta[h_E^{\mathrm{syn}}(\mathbf{x}, s)]\}$. If, now, $\phi_\beta[h_E^{\mathrm{syn}}(\mathbf{x}, t)]$ is small and slowly varying – which is à la Wilson and Cowan – then this probability may be written $1-\sum_{t-r_e<s\le t}\phi_\beta[h_E^{\mathrm{syn}}(\mathbf{x}, s)]$ and replaced by $1-r_e\phi_\beta[h_E^{\mathrm{syn}}(\mathbf{x}, t)]$. Thus we find

$$E(\mathbf{x}, t+\Delta t) = \{1-r_e\phi_\beta[h_E^{\mathrm{syn}}(\mathbf{x}, t)]\}\phi_\beta[h_E^{\mathrm{syn}}(\mathbf{x}, t)]\,. \tag{27}$$

Under the very same assumption we can rewrite this

$$E(\mathbf{x}, t+\Delta t) = \{1-r_e E(\mathbf{x}, t)\}\phi_\beta[h_E^{\mathrm{syn}}(\mathbf{x}, t)]\,. \tag{28}$$

In view of their very definition (26), activity E and its companion I can also enter $h_E^{\mathrm{syn}}(\mathbf{x}, t)$, originally a sum over the other j, so as to finally reappear in the form

$$h_E^{\mathrm{syn}}(\mathbf{x}, t) = \int ds d\mathbf{y}\, \varepsilon(s)\, \rho_E(\mathbf{y})\, J_{\mathrm{EE}}(\mathbf{x}-\mathbf{y})\, \mathcal{E}(\mathbf{x}, \mathbf{y}, t-s; \Delta) + \int ds d\mathbf{y}\, \varepsilon^{\mathrm{inh}}(s)\, \rho_I(\mathbf{y})\, J_{\mathrm{EI}}(\mathbf{x}-\mathbf{y})\, \mathcal{I}(\mathbf{x}, \mathbf{y}, t-s; \Delta)\,. \tag{29}$$

Here we have inserted, analogously to (16),

$$\mathcal{E}(\mathbf{x}, \mathbf{y}, t-s; \Delta) := E(\mathbf{y}, t-s-\Delta(\|\mathbf{x}-\mathbf{y}\|))\,,$$
$$\mathcal{I}(\mathbf{x}, \mathbf{y}, t-s; \Delta) := I(\mathbf{y}, t-s-\Delta(\|\mathbf{x}-\mathbf{y}\|))\,.$$

The continuum limit is important in that it allows us to define smooth deterministic averages such as E and I. Combining (28) and (29) we obtain the first of the two equations of Wilson and Cowan (1973):

$$\tau \frac{\partial E(\mathbf{x}, t)}{\partial t} = -E(\mathbf{x}, t) + \{1-r_e E(\mathbf{x}, t)\} \times \phi_{\beta,e}\left[\int ds d\mathbf{y} \varepsilon(s) \rho_E(\mathbf{y}) J_{\mathrm{EE}}(\mathbf{x}-\mathbf{y}) \mathcal{E}(\mathbf{x}, \mathbf{y}, t-s; \Delta) + \int ds d\mathbf{y} \varepsilon^{\mathrm{inh}}(s) \rho_I(\mathbf{y}) J_{\mathrm{EI}}(\mathbf{x}-\mathbf{y}) \mathcal{I}(\mathbf{x}, \mathbf{y}, t-s; \Delta)\right]\,. \tag{30}$$

The second follows in the very same manner:

$$\tau \frac{\partial I(\mathbf{x}, t)}{\partial t} = -I(\mathbf{x}, t) + \{1-r_i I(\mathbf{x}, t)\} \times \phi_{\beta,i}\left[\int ds d\mathbf{y}\, \varepsilon(s)\, \rho_E(\mathbf{y})\, J_{\mathrm{IE}}(\mathbf{x}-\mathbf{y})\, \mathcal{E}(\mathbf{x}, \mathbf{y}, t-s; \Delta) + \int ds d\mathbf{y} \varepsilon^{\mathrm{inh}}(s) \rho_I(\mathbf{y}) J_{\mathrm{II}}(\mathbf{x}-\mathbf{y}) \mathcal{I}(\mathbf{x}, \mathbf{y}, t-s; \Delta)\right]\,. \tag{31}$$

As usual, $\tau = \Delta t = 1$ ms. Without changing a single syllable we could generalize the above argument so as to allow the update ϕ to depend on the specific kind of neuron, here denoted by the subscripts e and i. Plainly, the very same holds true for (24) and (25). If desired, one can now perform a time coarse graining.

5 Symmetries

In uniform systems with constant densities ρ, the key equations (24) and (25) of Sect. 4 have quite a few *spatial* symmetries, which are determined by the convolution kernel(s) J and delays Δ. Usually these only depend on the distance [e.g., $J(\mathbf{x}-\mathbf{y}) = J(\|\mathbf{x}-\mathbf{y}\|)$] and, hence, exhibit the full two-dimensional rotation symmetry, as does the ordinary Lebesgue measure. Let us now imagine that we multiply the excitatory ε by a constant A that is to be considered as a bifurcation parameter. For (24) and (25) there exists a homogeneous stationary state $\mathcal{S}$, and one may wonder what kind of state bifurcates from $\mathcal{S}$ as A increases.

In principle – and forgetting about the delays – the underlying analysis has been done by Ermentrout and Cowan (1979), who took advantage of Sattinger's (1979, 1980, 1983) beautiful work on bifurcation at an eigenvalue whose (infinite) degeneracy stems from a spatial symmetry group. The only proviso of their analysis is that, roughly, the inhibition has so long a range that the patterns turn out to be stationary parallel stripes; in more recent terminology (Murray 1989), they find *Turing patterns*. Figures 1–4 do not belong to the Turing class so that some work remains to be done, the more so since delays such as $\Delta(\|\mathbf{x}-\mathbf{y}\|)$ had not been included yet. Moreover, e.g., the spirals of Fig. 2 rotate – in agreement with hallucination reports (Siegel and West 1975).

Does a bifurcation analysis starting from $\mathcal{S}$ solve the problem of determining all the spontaneous excitations? No, alas not. To see why, we return to the discrete case where we always started with the stationary state $\mathcal{S}$ of incoherently firing neurons and then let the system evolve under its own dynamics – given A. Scenarios II and III occur *long after* $\mathcal{S}$ has become unstable and greatly differ from scenario I, which bifurcates from $\mathcal{S}$. Of course, one could argue that it is A that determines what kind of excitation evolves out of the random initial state. So $\mathcal{S}$ might, but – as we have just seen – need not, carry the relevant information.

It is straightforward to determine $\mathcal{S}$ from the fixed-point equations

$$h_E^{\mathcal{S}} = c_1 \phi_\beta(h_E^{\mathcal{S}}) + c_2 \phi_\beta(h_I^{\mathcal{S}}) \tag{32}$$

and

$$h_I^{\mathcal{S}} = c_3 \phi_\beta(h_E^{\mathcal{S}}) + c_4 \phi_\beta(h_I^{\mathcal{S}}) \,. \tag{33}$$

The constants c_1–c_4 contain integrals over $J_{\mathrm{EE}}\varepsilon$ and η, $J_{\mathrm{EI}}\varepsilon^{\mathrm{inh}}$, $J_{\mathrm{IE}}\varepsilon$, and $J_{\mathrm{II}}\varepsilon^{\mathrm{inh}}$ and η, respectively. In passing we note that the bifurcation parameter A occurs in c_1 and c_3. State $\mathcal{S}$ is characterized by a stationary incoherent firing of the neurons and, thus, described uniquely by $h_E^{\mathcal{S}}$ and $h_I^{\mathcal{S}}$ as they follow from (32) and (33).

6 Orientation preference

Many neurons have a direction selectivity in the sense that they prefer a certain direction more strongly than others. We now indicate how one can incorporate this orientation preference of neuronal cells in a simple manner. Thanks to optical imaging (Bonhoeffer and Grinvald 1991, 1993), direction selectivity is now known in rather great detail. It has been shown that iso-orientation domains are small patches organized in so-called pinwheels around orientation centers, singularities. In cat visual cortex their density is $1.2\,\mathrm{mm}^{-2}$. Furthermore, the direction changes *continuously* – except at the singularities. For a given singularity and rotation (clockwise or counterclockwise) structure, the field $\mathbf{n}$ of preferred direction is more or less fixed. We therefore assume that $\mathbf{n}(\mathbf{x})$ is a given function of position $\mathbf{x}$ in the primary visual cortex. Neurons with the same orientation interact excitatorily; those with different orientation preferences inhibit each other. This is not a shunting inhibition. It does not contradict Dale's principle, either, as the inhibition is delivered via interneurons. Then the synaptic strength between neurons at $\mathbf{x}$ and those at $\mathbf{y}$ with preferred directions $\mathbf{n}(\mathbf{x})$ and $\mathbf{n}(\mathbf{y})$ is a smooth function K of, say, the scalar product $\mathbf{n}(\mathbf{x}) \cdot \mathbf{n}(\mathbf{y})$. Note that $\mathbf{n}$ is a unit vector. We have $K(1) = 1$; K is decreasing fast to negative values (or zero, depending on the modeling) once we move away from $x = 1$, and it depends on the local situation (e.g., Bonhoeffer and Grinvald 1991, 1993) whether $K(-1) \approx K(1)$ or $K(-1) < 0$. In (24) we now assume $J_{\mathrm{EE}} \geq 0$ and perform the substitution

$$J_{\mathrm{EE}} \to J_{\mathrm{EE}}\, K(\mathbf{n}(\mathbf{x}) \cdot \mathbf{n}(\mathbf{y})) \,. \tag{34}$$

It must be constantly borne in mind, however, that $\mathbf{n}(\mathbf{x})$ is a *given* vector field. As for the rest, no essential changes are expected to be necessary. Direction selectivity may strongly modify the elementary excitation patterns, as is brought out clearly by the figures of Kistler et al. (1998).

7 Discussion

The aim of the present paper was to show two things. First, though neurons are to be modeled as stochastic elements, the strong law of large numbers (Breiman 1968) allows for a strong data reduction *in the continuum limit*. One has to verify, however, whether this limit is allowed. Under rather mild conditions as specified in Sect. 4, it is.

In fact, the argument is simple and straightforward and also allows a derivation of classical results such as those of Wilson and Cowan, thus showing under what conditions they are valid. The continuum limit transforms a discrete system of neurons into an "excitable" medium. This medium is described by the hillock potential $h(\mathbf{x}, t)$, where $\mathbf{x}$ and t represent space and time, continuous variables. In a cortical context, the quantity h contains global input from many ($\approx 10^4$) neighbors. Neurons exhibiting refractoriness have a memory, a *local* one. We therefore needed some smoothing of the local refractory behavior so as to transform it into a function of h.

The second issue is a far more subtle one, viz., the role of noise as time proceeds. A large system of discrete noisy neurons may asymptotically behave in a way *not* predicted by continuous equations such as (24) and (25). As for scenario IV starting from the (unstable) homogeneous fixed point, one can simply add some noise by hand or, simulating it, wait for a numerical instability. Discrete structures, however, may break up as $t \to \infty$. That is, they are *fragile*. This is nicely illustrated by Fig. 5, where rings, which have a *finite* thickness, are not stable and break up as they grow. Because the rings are discrete and growing, it is simply a matter of time before a hole appears in a ring of finite thickness and the ring opens up and forms a stripe. In scenario IV small sets of noisy neurons ignite the system; in scenario I small noisy holes, *non*active neurons, destroy coherence. Hence describing noise seems to be a separate problem and makes the answer to the question raised in the abstract, "Does the continuum limit present a full description of scenarios found numerically?"a biological one: No, not quite.

Does all this contradict the limit theorem of Sect. 4? The answer is a simple no. In mathematical terms, an interchange of the continuum limit $a \to 0$ in conjunction with $\Delta t \to 0$ and the limit $t \to \infty$ is not allowed. For practical work, however, discrete structures being fragile greatly restrains the applicability of the limit theorem – that is to say, valuable as it may be, it should not be overestimated.

Equipped with the benefit of hindsight, the reader might wonder whether the present approach is consistent with analyses leading to partial differential equations of the Fitzhugh–Nagumo or similar type, which one can immediately write down (Murray 1989, §12.4). Indeed one can, but they do not describe a true neuronal system. Typically, one has a variable u representing the membrane

potential and a "refractory" variable v. The interaction with other neurons is taken into account by a Laplacian, a strictly local operator. Postsynaptic potentials do not appear, and thus it is impossible to describe their essential role in generating stable coherent excitations (Gerstner et al. 1996). So the way in which spikes convey information is not considered at all. Furthermore, noise has not been included, either. In short, this continuum description is far from being complete.

It is to be noted that a "discretization" of the delay integrodifferential equations derived here is a completely different affair. The discrete structure we started with had single neurons as noisy elements that were updated independently of each other. This rule is in agreement with the underlying biophysics. A numerical discretization starts with a *continuous* structure and divides, say, function ϕ into several slices. Two neighboring slices, however, are similar, whereas two neighboring neurons may behave in a completely opposite way by firing and *not* firing, despite the same input. So it looks as if Nature gives rise to a richer behavior and our conclusion is to be: Cortical tissue is not quite an excitable medium.

Acknowledgements. The author gratefully acknowledges the hospitality of R.M. May at the Department of Zoology of the University of Oxford, where this work was started, and of Jack D. Cowan at the Department of Mathematics of the University of Chicago, where the manuscript took its final shape. His visit to Oxford was made possible by EC Grant ERB CHRX-CT92-0063, and financial support from the Department of Mathematics of the University of Chicago was indispensable to his stay there. The author thanks Andreas Herz (Oxford) for explaining to him the $\Sigma - \Pi$ exchange and Bard Ermentrout (Pittsburgh) for pointing out where it came from. He is grateful to Maarten Boerlijst (Oxford) for some helpful advice and Wulfram Gerstner (TU München) in 1994 for a most enjoyable collaboration on the various issues discussed here. Finally, it is a great pleasure to thank Jack Cowan, Wulfram Gerstner, Uwe an der Heiden (Witten/Herdecke), and Bernhard Sulzer (Los Alamos) for a critical reading of the manuscript and helpful suggestions, and Corinna Fohlmeister (now Raab) for having made available the pictures of Fig. 5 stemming from her diploma thesis (Fohlmeister 1994).

References

Bonhoeffer T, Grinvald A (1991) Iso-orientation domains in cat visual cortex are arranged in pinwheel-like patterns. Nature 353:429–431

Bonhoeffer T, Grinvald A (1993) The layout of iso-orientation domains in area 18 of cat visual cortex: optical imaging reveals a pinwheel-like organization. J Neurosci 13:4157–4180

Braitenberg V, Schütz A (1991) Anatomy of the cortex: statistics and geometry. Springer, Berlin Heidelberg New York

Breiman L (1968) Probability. Addison-Wesley, Reading, MA (Sect. 3.6)

Cowan JD (1968) Statistical mechanics of nervous nets. In: Caianiello ER (ed) Neural networks. Springer, Berlin Heidelberg New York, pp 181–188

Cowan JD (1985) What do drug-induced visual hallucinations tell us about the brain? In: Levy WB, Anderson JA, Lehmkuhle S (eds) Synaptic modification, neuron selectivity, and nervous system organization. Erlbaum, Hillsdale, NJ, pp 223–241

Cross MC, Hohenberg PC (1993) Pattern formation outside of equilibrium. Rev Mod Phys 65:851–1112

Ermentrout G, Cowan JD (1979) A mathematical theory of visual hallucination patterns. Biol Cybern 34:137–150

Ermentrout GB, Cowan JD (1979) Temporal oscillations in neuronal nets. J Math Biol 7:265–28

Ermentrout GB, Cowan JD (1980) Large scale spatially organized activity in neural nets. SIAM J Appl Math 38:1–21 [especially Eqs. (1.6)–(1.8)]

Feldman JL, Cowan JD (1975) Large-scale activity in neural nets: I. Theory with applications to motoneuron pool responses. Biol Cybern 17:29–38 (see in particular mathematical appendix)

Fohlmeister C (1994) Modellierung von Halluzinationen im visuellen Cortex. Diploma thesis, Physik Department, Technische Universität München

Fohlmeister C, Ritz R, Gerstner W, van Hemmen JL (1995) Spontaneous excitations in the visual cortex: stripes, spirals, rings, and collective bursts. Neural Comput 7:905–914

Gerstner W (1995) Time structure of the activity in neural network models. Phys Rev E 51:738–758

Gerstner W, van Hemmen JL (1992) Associative memory in a network of 'spiking' neurons. Network 3:139–164

Gerstner W, van Hemmen JL (1993) Coherence and incoherence in a globally coupled ensemble of pulse-emitting units. Phys Rev Lett 71:312–315

Gerstner W, van Hemmen JL (1994) Coding and information processing in neural networks. In: Domany E, van Hemmen JL, Schulten K (eds) Models of neural networks II. Springer, Berlin Heidelberg New York (Chap 1)

Gerstner W, Ritz R, van Hemmen JL (1993) A biologically motivated and analytically soluble model of collective oscillations in the cortex: I. Theory of weak locking. Biol Cybern 68: 363–374

Gerstner W, van Hemmen JL, Cowan JD (1996) What matters in neuronal locking? Neural Comput 8:1689–1712

An der Heiden U (1980) Analysis of neural networks. Springer, Berlin Heidelberg New York

Hessler NA, Shirke AM, Mallnow R (1993) The probability of transmitter release at a mammalian central synapse. Nature 366:569–572

Hopfield JJ (1984) Neurons with graded response have computational properties like those of two-state neurons. Proc Natl Acad Sci USA 81:3088–3092

Kandel ER, Schwartz JH, (eds) (1985) Principles of neural science, 2nd edn. Elsevier, New York

Kistler W, Gerstner W, van Hemmen JL (1997) Reduction of Hodgkin–Huxley equations to single-variable threshold model. Neural Comput 9:1015–1045

Kistler WM, Seitz R, van Hemmen JL (1998) Modeling collective excitations in cortical tissue. Physica D 114:273–295

Klüver H (1966) Mescal and the mechanisms of hallucination. University of Chicago Press, Chicago (especially pp 65–80)

Lamperti J (1966) Probability. Benjamin, New York

Levin SA, Segel LA (1985) Pattern generation in space and aspect. SIAM Rev 27:45–67

Meron E (1992) Pattern formation in excitable media. Phys Rep 218:1–66

Milton JG, Mundel T, an der Heiden U, Spire J-P, Cowan JD (1995) Activity waves in neural networks. In: Arbib MA (ed) The handbook of brain theory and neural networks. MIT Press, Cambridge, MA

Murray JD (1989) Mathematical biology. Springer, Berlin Heidelberg New York (especially pp 161–166, 328–335, 481–505)

Riedel U, Kühn R, van Hemmen JL (1988) Temporal sequences and chaos in neural nets. Phys Rev A 38:1105–1108

Rosenmund C, Clements JD, Westbrook G (1993) Nonuniform probability of glutamate release at a hyppocampal synapse. Science 262:754–757

Sattinger DH (1979) Group theoretic methods in bifurcation theory. Lecture notes in mathematics, vol 762. Springer, Berlin Heidelberg New York

Sattinger DH (1980) Symmetry breaking and bifurcation in applied mathematics. Bull Am Math Soc 3:779–819

Sattinger DH (1983) Branching in the presence of symmetry. SIAM, Philadelphia

Sholl DA (1956) The organization of the cerebral cortex. Wiley, New York

Siegel RK, West LJ (1975) Hallucinations: behavior, experience, and theory. Wiley, New York

Siegel RK (1977) Hallucinations. Sci Am 237(4): 132–140

Tyson JJ, Keener JP (1988) Singular perturbation theory of traveling waves in excitable media (a review). Physica D 32: 327–361

Wilson HR, Cowan JD (1973) A mathematical theory of the functional dynamics of cortical and thalamic nervous tissue. Kybernetik 13:55–80 [especially Eqs. (1.3.1) and (1.3.2)]